RSC Advances

PAPER

View Article Online
View Journal | View Issue

Cite this: *RSC Adv.*, 2022, **12**, 23322

Halogen-free layered double hydroxide-cyclotriphosphazene carboxylate flame retardants: effects of cyclotriphosphazene di, tetra and hexacarboxylate intercalation on layered double hydroxides against the combustible epoxy resin coated on wood substrates†

Velusamy Jeevananthan and Swaminathan Shanmugan *

The development of halogen-free flame retardants as environmentally friendly and renewable materials for heat and fire-resistant applications in the field of electronics is important to ensure safety measures. In this regard, we have proposed a simple and halogen-free strategy for the synthesis of flame retardant LDH-PN materials to decrease the fire hazards of epoxy resin (EP), *via* a co-precipitation reaction between $Mg(NO_3)_2$ and $Al(NO_3)_3$ and the subsequent incorporation of different cyclotriphosphazene (PN) carboxylate anions. The cyclotriphosphazene-based di, tetra and hexacarboxylate-intercalated layered double hydroxides are designated as LDH-PN-DC, LDH-PN-TC and LDH-PN-HC, respectively. Furthermore, the intercalation of cyclotriphosphazene carboxylate anions into the LDH layers was confirmed by PXRD, FT-IR, TGA, solid-state ^{31}P NMR, nitrogen adsorption and desorption analysis (BET), HR-SEM and XPS. Evaluation of the flame retardant (vertical burning test and limiting oxygen index) properties was demonstrated by formulating the LDH-PN materials with epoxy resin (EP) in different ratios coated on wood substrates to achieve the desired behaviour of the EP/LDH-PN composites. Structure–property analysis reveals that EP/LDH-PN-TC-20 wt% and EP/LDH-PN-HC-20 wt% achieved a V_0 rating in the UL-94 V test and achieved higher LOI values (27.7 vol% for EP/LDH-PN-TC-20 wt% and 29 vol% for EP/LDH-PN-HC-20 wt%) compared to the epoxy-coated wood substrate (23.2 vol%), whereas EP/LDH-PN-DC failed in the vertical burning test for various weight percentages of LDH-PN-DC from 5 wt% to 20 wt% in the composites, with a lower LOI value of 22.1 vol%. Excellent flame retardancy was observed for EP/LDH-PN-TC and EP/LDH-PN-HC due to the presence of more binding sites of carboxylate anions in the LDH layers and less or no spiro groups in cyclotriphosphazene compared to that in EP/LDH-PN-DC. In addition, the synergistic flame retardant effect of the combination of LDH and cyclotriphosphazene on the epoxy resin composites remains very effective in creating a non-volatile protective film on the surface of the wood substrate to shelter it from air, absorb the heat and increase the ignition time, which prevents the supply of oxygen during the combustion process. The results of this study show that the proposed strategy for designing flame-retardant properties represents the state-of-the-art, competent coating of inorganic materials for the protection and functionalization of wood substrates.

Received 23rd April 2022
Accepted 29th July 2022

DOI: 10.1039/d2ra02586h

rsc.li/rsc-advances

Introduction

Technical combustion processes are indispensable for the industrialized world to generate power in different forms such as mechanical energy, electrical energy and heat energy. However, fire-related accidents are an impairment of human lives and have social and environmental costs. As a result, combustible materials such as wood, fabrics and synthetic polymers are frequently preserved with flame retardants to suppress fire discharges and tragedies. Flame retardant materials inhibit fire development and propagation, and thereby reduce economic damage and help to protect human lives.[1] Halogen-containing flame retardant materials display satisfactory fire resistance in a polymer matrix and have been widely used to overcome flammability.[2,3] Unfortunately, the presence of halogen-containing flame retardant materials may release toxic gases and corrosive fumes during combustion processes,

Department of Chemistry, Faculty of Engineering and Technology, SRM Institute of Science and Technology, Kattankulathur 603203, Tamil Nadu, India. E-mail: shanmugs2@srmist.edu.in; shanmugan0408@gmail.com

† Electronic supplementary information (ESI) available. See https://doi.org/10.1039/d2ra02586h

which may cause health and environmental hazards.[4,5] Therefore, it is important to develop eco-friendly halogen-free intumescent flame retardant materials to enrich the safety measures. Inorganic flame retardants are a fast-growing class of halogen-free flame retardants, which include antimony oxide, magnesium hydroxide and aluminium hydroxide, and the main drawback of these flame retardants is that a very high loading is required to attain satisfactory flame retardant ratings for the final products.[6]

In recent years, layered double hydroxides (LDHs) have received much attention in the synthesis of the halogen-free flame retardants due to their non-toxicity, low cost, high thermal stability, adjustable chemical composition, unique layered structure, and exchangeable interlayer anions.[7,8] LDHs are layered materials made of positively charged metal hydroxide sheets, negatively charged anions and water molecules at the gallery to balance the charge.[9] The general chemical formula of LDHs can be illustrated as $[M^{2+}_{1-x}\ M^{3+}_{x}(OH)_2]^{x+}[A^{n-}_{x/n}]\cdot mH_2O$, where M^{2+} and M^{3+} are divalent and trivalent metal cations, respectively, and A^{n-} are the interlayer anions. Strong interlayer electrostatic interactions are caused between the LDH sheets due to the high charge density of the LDH layers, high content of anionic species and water molecules representing hydrophilic properties.[10] Because of these properties, it is desirable that pristine LDHs be altered by the intercalation of different types of organic modifiers to modify their surface and interior properties by weakening the electrostatic forces between the LDH sheets, increasing the interlayer distance of LDHs for the penetration of larger polymers and making the LDHs organophilic.[11] A wide range of organic modifiers such as carboxylates, phosphonates and sulfonates have been utilized to alter the surface properties of LDHs.[12,13] Most of the modified LDHs, such as LDH-long-chain linear alkyl carboxylates and sulfonates, are used as flame retardant additives for blending with low-density polyethylene, polypropylene, poly(methyl methacrylate), polystyrene and poly(L-lactide) to yield LDH-polymer nanocomposites.[14,15] During the combustion process, the flame retardant property of LDH-polymer composites can contribute by absorbing heat, increasing the ignition time, releasing aqueous vapour, reducing combustible gases during pyrolysis and producing an oxide layer on the surface of the material, which can prevent further degradation.[16,17]

Besides organic modifiers in LDHs, inorganic anions such as phosphates and borates are intercalated in LDH layers and used as flame retardant additives as the synergistic effect between the phosphates or borates equally distributed in the interlayer region and the host LDH layers reduces the rate of heat release and the fire growth rate index compared to the LDH carbonate or sulphate precursors.[18,19] As the mainly used compound, cyclotriphosphazene is a versatile inorganic ring compound in which phosphorous and nitrogen atoms are arranged in alternating positions and two chlorine atoms are attached to each phosphorous atom, which is reactive to different nucleophiles, offering synthetic flexibility to introduce desirable functionalities that can subsequently be transformed into desired synthetic precursors.[20,21] Cyclotriphosphazene and its derivatives have been commonly used as halogen-free flame retardants owing to their high reactivity, non-toxic nature, high thermal stability, excellent flame retardant efficiency and self-extinguishability that are brought about by their unique molecular design of a PN ring structure.[22–24] Several substituted cyclotriphosphazenes have been reported so far to develop potential flame retardants with enhanced thermal stability using two different approaches: (i) the first approach is the blending of different substituents on the aryl group of hexaphenoxycyclotriphosphazene with thermosetting polymers[25–29] and (ii) the second approach is the synthesis of different crosslinked cyclomatrix phosphazene polymers and cyclolinear and spirocyclic phosphazene epoxy resins using cyclotriphosphazene with desired functional groups.[30–36] Due to the endothermic decomposition of cyclotriphosphazene polymers, the non-volatile protective films on the surface of the polymeric materials are generated to insulate them from air; concurrently, non-flammable gases are also released, which stop the oxygen supply.[37–39] Recently, the effects of the addition of nickel–iron, nickel–aluminium, and nickel–chromium LDH-sodium dodecyl sulfate (LDH-SDS) and hexaphenoxycyclotriphosphazene (HPCP) on the poly(lactic acid) (PLA) matrix to produce PLA/HPCP/LDH-SDS composites by the melt mixing method have been suggested, and the different types of LDH-SDS materials show the important function of enhancing the thermal stability and flame retardancy of PLA composites by reducing the mass and heat transfer between the gas and condensed phases. Furthermore, the modified nickel–cobalt metal layered double hydroxide with polyphosphazene produces the Ni–Co-LDH@PZS architecture for the application of high fire safety, especially the suppression of smoke and toxic gases during epoxy resin burning.[40] To the best of our knowledge, there is no report on the intercalation of cyclotriphosphazene carboxylate anions into LDH layers and its application in flame retardancy. Therefore, the combination of both LDH and cyclotriphosphazene through non-covalent bonding will produce LDH-PN materials possessing superior flame retardancy by increasing the interlayer distance of the LDH layers for the dispersion of polymers such as epoxy resin. Based on the above discussion, three cyclotriphosphazene carboxylate anion-intercalated Mg–Al-LDH materials, represented as LDH-PN materials, were synthesized and characterized. Then, the LDH-PN materials were incorporated into epoxy resin with different loadings using ultrasonication and thermal curing processes, which were then coated on a wood substrate. Subsequently, the flame retardancy of the EP/LDH-PN composite-coated wood substrates was estimated using the vertical burning test (UL 94 V) and limiting oxygen index (LOI) test. Excellent flame retardancy was observed for EP/LDH-PN-TC-20 wt% and EP/LDH-PN-HC-20 wt% in the UL 94 V test, and they displayed high LOI values (27.7 vol% for EP/LDH-PN-TC-20 wt% and 29 vol% for EP/LDH-PN-HC-20 wt%), whereas both epoxy resin and EP/LDH-PN-DC-20 wt% failed in the UL 94 V test and showed low oxygen concentration in the LOI test (23.2 vol% for epoxy resin and 22.1 vol% for EP/LDH-PN-DC-20 wt%).

Experimental section

Materials and methods

All chemicals were of analytical grade and used without further purification. Hexachlorocyclotriphosphazene (Sigma Aldrich), 2,2′-biphenol (Sigma Aldrich) and methyl 4-hydroxybenzoate (AVRA) were recrystallized from *n*-hexane, dichloromethane and acetone, respectively. Acetone, used as a solvent in the reactions, was pre-distilled with $KMnO_4$ and further distilled with anhydrous K_2CO_3. Commercially available chemicals such as $Al(NO_3)_3\cdot 9H_2O$ (Merck), $Mg(NO_3)_2\cdot 6H_2O$ (SRL), 2,2-bis(4-glycidyloxyphenyl) propane (TCI) as epoxy resin, and triethylenetetramine (TETA) (SRL) were used as received. Deionized water was employed in the hydrolysis reactions and LDH synthesis. dispiro-$N_3P_3(O_2C_{12}H_8)_2Cl_2$ (**1**), spiro-$N_3P_3(O_2C_{12}H_8)Cl_4$ (**3**)[41,42] and $N_3P_3(OC_6H_4COOH)_6$ ($\mathbf{L_3}$)[43] were synthesized according to the reported procedures. The detailed synthetic procedures of [dispiro-$N_3P_3(O_2C_{12}H_8)_2(OC_6H_4COOH)_2$] ($\mathbf{L_1}$) and [spiro-$N_3P_3(O_2C_{12}H_8)(OC_6H_4COOH)_4$] ($\mathbf{L_2}$) are given in the ESI.† The Fourier transform infrared (FT-IR) spectra were examined on a Shimadzu IR Tracer-100 in the range of 400 to 4000 cm^{-1}. Nuclear magnetic resonance (^1H, ^{13}C and ^{31}P) spectroscopy was carried out using a Bruker Advance DPX-250 spectrometer operating at 500 MHz. Electrospray ionization mass spectrometry (ESI-MS) was performed on a Shimadzu LC-MS 2020 spectrometer equipped with an LC10ADVP binary pump. The changes in crystallinity were observed using powder X-ray diffractometry (PXRD, PANalytical India, Spectris Technologies) with Cu Kα radiation ($\lambda = 1.54$ Å) in the range of 5° to 100°. The thermal stability and weight loss were studied by thermogravimetric analysis (TGA) using a Netzsch-STA 2500 Regulus instrument at a heating rate of 10 °C per min under a nitrogen atmosphere. The morphology of the samples was observed using high-resolution scanning electron microscopy (HR-SEM, Thermosceintific Apreo S). The surface area of the samples was measured by the Brunauer–Emmett–Teller (BET) method on a Quantachrome Autosorb iQ sorption analyzer. The chemical composition was studied by X-ray photoelectron spectroscopy (XPS) using a ULVAC-PHI, PHI5000 Version Probe III, Physical Electronics instrument. The flame retardant properties were examined by the vertical burning test (UL-94 V), and limiting oxygen index (LOI) tests were carried out on a Stanton Red Croft FTT.

Synthesis of cyclotriphosphazene carboxylate anion-intercalated LDH (LDH-PN)

Synthesis of cyclotriphosphazene dicarboxylate anion-intercalated LDH (LDH-PN-DC). The matched molar ratio of Mg^{2+}/Al^{3+}/cyclotriphosphazene dicarboxylic acid was 4 : 2 : 1. A solution of $Mg(NO_3)_3\cdot 6H_2O$ (7.72 mmol) and $Al(NO_3)_3\cdot 9H_2O$ (3.86 mmol) in 20 ml deionized water was slowly added to a 30 ml aqueous solution of NaOH (0.1 N) and cyclotriphosphazene dicarboxylic acid ($\mathbf{L_1}$) (1.93 mmol) with vigorous stirring under N_2 atmosphere, and the value of the pH was adjusted to above 10 by adding a 1 M NaOH solution. The resulting slurry was aged at 70 °C for 36 h, centrifuged, washed with deionized water until pH = 7.0, and dried at 70 °C for 2 days. The final dried solid was crushed with a mortar and pestle to produce a fine powder. Yield: 2.2 g. IR (ATR, cm^{-1}): 3420(b), 1599(s), 1535(s), 1499(m), 1474(m), 1438(m), 1384(s), 1272(s), 1231(s), 1216(m), 1160(s), 1093(s), 937(s), 885(s), 780(s), 749(s), 717(m), 665(s), 604(s), 563(m), 540(m). Solid-state ^{31}P NMR (162 MHz) δ (ppm): 29.0 ($[C_{12}H_8O_2]_2$, 2P), 10.4 ($[C_7H_4O_3]_2$, 1P). TGA: temperature range (weight loss): 70–215 °C (9.2%), 230–720 °C (40.9%) and 800–1000 °C (4.7%).

Synthesis of cyclotriphosphazene tetracarboxylate anion-intercalated LDH (LDH-PN-TC). LDH-PN-TC was prepared by a similar synthetic procedure as LDH-PN-DC using cyclotriphosphazene tetracarboxylic acid ($\mathbf{L_2}$) instead of cyclotriphosphazene dicarboxylic acid ($\mathbf{L_1}$). The matched molar ratio of Mg^{2+}/Al^{3+}/cyclotriphosphazene tetracarboxylic acid ($\mathbf{L_2}$) was 8 : 4 : 1 (13.83 mmol : 6.92 mmol : 1.73 mmol). Yield: 2.1 g. IR (ATR, cm^{-1}): 3401(b), 1599(s), 1555(s), 1544(m), 1500(m), 1384(s), 1271(m), 1212(m), 1160(s), 1159(s), 1095(s), 1013(m), 970(s), 883(m), 780(m), 754(b), 665 (s), 606(s), 553(s). Solid-state ^{31}P NMR (162 MHz) δ (ppm): 28.0 ($C_{12}H_8O_2$, 1P), 12.9 ($[C_7H_4O_3]_4$, 2P). TGA: temperature range (weight loss): 70–230 °C (15.5%), 230–720 °C (28.6%) and 800–1000 °C (4.7%).

Synthesis of cyclotriphosphazene hexacarboxylate anion-intercalated LDH (LDH-PN-HC). LDH-PN-HC was also prepared by a similar synthetic procedure as LDH-PN-DC using cyclotriphosphazene hexacarboxylic acid ($\mathbf{L_3}$) instead of cyclotriphosphazene dicarboxylic acid ($\mathbf{L_1}$). The matched molar ratio of Mg^{2+}/Al^{3+}/cyclotriphosphazene hexacarboxylic acid ($\mathbf{L_3}$) was 12 : 6 : 1 (18.80 mmol : 9.40 mmol : 1.57 mmol). Yield: 3.2 g. IR (ATR, cm^{-1}): 3307(b), 1599(s), 1540(s), 1499(m), 1384(s), 1268(m), 1208(m), 1160(s), 1097(m), 1014(m), 970(s), 883(m), 789(m), 736(m), 665(s), 595(m), 558(m). Solid-state ^{31}P NMR (162 MHz) δ (ppm): 12.7 ($[C_7H_4O_3]_6$, 3P). TGA: temperature range (weight loss): 70–230 °C (15.0%), 230–720 °C (29.0%) and 800–1000 °C (4.2%).

Preparation of the EP/LDH-PN composites. The EP/LDH-PN composites were prepared by a previously reported procedure with some modification.[44,45] All three LDH-PN materials with different weight percentages (5 wt%, 10 wt%, 15 wt%, and 20 wt%) were dispersed in DMF using sonication for an hour. The desired amount of epoxy resin was added to the LDH-PN suspension and sonicated for an hour. Then, DMF was removed by a vacuum-assisted rota-evaporator and the resultant slurry was mixed at 120 °C for ten minutes. After reaching room temperature, the desired amount of curing agent (TETA) was added to the EP/LDH-PN mixture, which was mixed under sonication for 3 minutes. Likewise, the epoxy resin sample was prepared by the above procedure without the addition of LDH-PN.

Preparation of the EP/LDH-PN wood substrate and brush coating. To improve the adhesion, all the teak wood substrates were treated with electro-coated SiC grain emery paper of 220 grit size before the coating of the EP/LDH-PN composites. After mixing the curing agent, the EP/LDH-PN composites were immediately coated on the wood substrates using flat brushes. Then, the EP/LDH-PN wood substrates were cured at room temperature for 24 hours and post-cured at 80 °C overnight.

Results and discussion

Synthesis and characterization

Several layered inorganic solids have been used as host materials for the construction of inorganic–organic host–guest supramolecular structures by intercalating guest molecules or ions. The LDH-PN materials were synthesized by the homogeneous co-precipitation reaction between $Mg(NO_3)_2$ and $Al(NO_3)_3$, followed by the intercalation of different cyclotriphosphazene (PN) carboxylate anions (Scheme 1).[46] For convenience, the PN-based dicarboxylic, tetracarboxylic and hexacarboxylic anion-intercalated LDHs were labelled LDH-PN-DC, LDH-PN-TC and LDH-PN-HC, respectively. The successful formation of the LDH-PN materials was confirmed by powder X-ray diffraction, FT-IR, thermogravimetric analysis, solid-state ^{31}P NMR, nitrogen adsorption and desorption analysis (BET), high-resolution scanning electron microscopy and X-ray photoelectron spectroscopy.

The powder XRD patterns of Mg–Al–NO_3-LDH, the three cyclotriphosphazene carboxylic acids ($\mathbf{L_1}$, $\mathbf{L_2}$, and $\mathbf{L_3}$) and the LDH-PN materials are shown in Fig. 1. The XRD patterns of the LDH-PN-DC, LDH-PN-TC and LDH-PN-HC materials confirm the formation of the LDH phase.[12,47,48] Bragg peaks of each pattern at the lower angle region of $2\theta < 25^\circ$ emerge from the reflections of the basal plane passing through the metal sites in the hydroxide layers.[49] Generally, the $d_{(003)}$ peak is known as the basal spacing of each layer in LDH, which is defined as the total distance of the interlayer and thickness of the hydroxide layer (4.8 Å).[50,51]

Comparing Mg–Al–NO_3-LDH with the LDH-PN materials, the basal *d*-spacings of LDH-PN-DC, LDH-PN-TC and LDH-PN-HC are shifted from 7.7 Å to 15.4 Å, 10.8 Å, and 10.7 Å, respectively. The increase in the *d*-spacing shows the successful intercalation of the cyclotriphosphazene carboxylate anions into the LDH layers, which makes the basal reflection of the acid-intercalated LDHs appear at a lower angle. In all the acid-intercalated LDHs, some of the carboxylic acid peaks are also present below the region of $2\theta = 30^\circ$.

The last diffraction peak ($d_{(110)}$) of $2\theta \simeq 60.8^\circ$ is responsible for the structural integrity of the LDH layers and was still maintained in all the acid-intercalated LDHs.[52] In addition, the $d_{(110)}$ spacing is related to the average distance between two metal ions in the hydroxide layers ($a_{M-M} = 2d_{(110)}$), which is calculated to be 3.04 Å for the LDH-PN materials and is almost equal to the average distance between Mg–Al in Mg–Al–NO_3-LDH (3.06 Å), with a metal fraction of 2. Thus, there is no significant change in the Mg–Al ratio, which indicates the complete precipitation of metal ions in the LDH-PN materials.[53]

Fig. 2a shows the FT-IR spectra of the LDH-PN-DC, LDH-PN-TC and LDH-PN-HC materials. In the spectra of all the LDH-PN materials, the broad band in the range of 3100–3600 cm^{-1} is attributed to the hydroxyl group stretching vibrations in the LDH layers and water molecules due to the formation of hydrogen bonding between the interlayer water and hydroxyl groups of the host layers and the guest anions. The band around 665 cm^{-1} is assigned to the stretching vibration of M–O in the hydroxide layers.[53,54] The characteristic band around 1160 cm^{-1} is ascribed to the P=N stretching vibration of the cyclotriphosphazene rings. The absorption bands around 970 cm^{-1} for LDH-PN-TC and LDH-PN-HC and 937 cm^{-1} for LDH-PN-DC are assigned to the P–O–C stretching vibration for the aromatic groups connected to the cyclic phosphorous atoms.[55] The strong absorption bands around 1590 cm^{-1} and 1380 cm^{-1} are assigned to the asymmetric and symmetric stretching vibrations of the $-COO^-$ groups, which shows that the carboxylic groups in the cyclotriphosphazenes are deprotonated to form their corresponding anions, indicating the successful intercalation of cyclotriphosphazene carboxylate anions into the LDH layers.[56]

The thermal stability, degradation behaviour and char formation ability of the LDH-PN and Mg–Al–NO_3-LDH materials were studied by thermogravimetric analysis. As depicted in Fig. 2b, the whole thermal degradation process consists of three steps: the first step displays the loss of both physically adsorbed and interlayered water molecules around the temperature range of 70–230 °C.[57–59] The percentages of weight loss for LDH-PN-DC, LDH-PN-TC, LDH-PN-HC and Mg–Al–NO_3-LDH in the first step are about 9.2%, 15.5%, 15.0% and 7.8%, respectively. The second step involves simultaneous dehydroxylation in the LDH layers and the decomposition of the organic groups attached with cyclotriphosphazene in the intercalated acid anions around the temperature range of 230–720 °C.[60] The percentages of weight loss in the second step for LDH-PN-DC, LDH-PN-TC, LDH-PN-HC and Mg–Al–NO_3-LDH are about 40.9%, 28.6%, 29.0% and 26.3%, respectively. In addition, the percentages of weight loss in the first and second steps for LDH-PN-TC and LDH-PN-HC are almost the same but different from those of the LDH-PN-DC material. The final step shows the minimum weight loss of around <5% for the LDH-PN materials, and gives a higher char yield (45.2% for LDH-PN-DC, 51.2% for LDH-PN-TC and 51.8% for LDH-PN-HC) in the range of 800 to 1000 °C. It could be assumed that cross-linking reactions occur during pyrolysis, comprising the ring-opening polymerization reaction of the cyclotriphosphazene structure[34,61] as well as the formation of a mixture of MgO and $MgAl_2O_4$ from the thermal degradation of the LDH layers as the final decomposition products.[62,63]

In the solution-state ^{31}P NMR spectra of $\mathbf{L_1}$ and $\mathbf{L_2}$, two observed signals around 9.0 and 25.0 ppm are attributed to the phosphorous atoms in cyclotriphosphazene attached to the phenoxy groups and spiro groups, respectively (Fig. S7 and S15†).[64] For the compound $\mathbf{L_3}$, only one singlet at 8.0 ppm is ascribed to the phosphorous atoms attached to the phenoxy groups, which indicates that all the phosphorous atoms in $\mathbf{L_3}$ remain magnetically equivalent.[43] Similarly, the solid-state ^{31}P NMR spectra of LDH-PN-DC and LDH-PN-TC display two signals (10.4 and 29.0 ppm for LDH-PN-DC; 12.9 and 28.0 ppm for LDH-PN-TC), and LDH-PN-HC shows only one signal at 12.7 ppm, as shown in Fig. 3a–c.[65] Thus, the solid-state ^{31}P NMR spectra of the LDH-PN materials are quite similar to those of their corresponding cyclotriphosphazene precursors, demonstrating that the cyclotriphosphazene carboxylate anions are

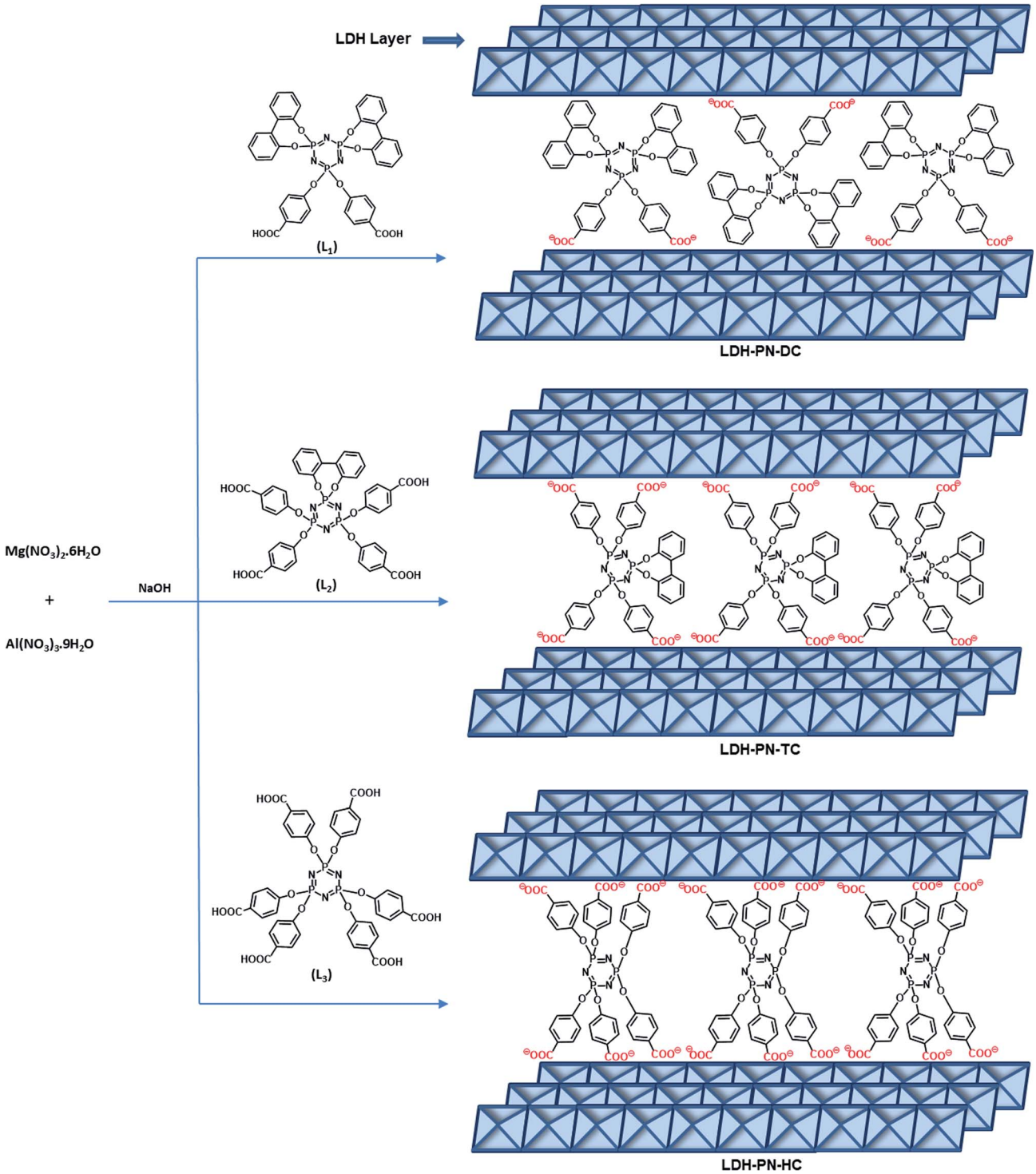

Scheme 1 Synthesis of cyclotriphosphazene carboxylate anion-intercalated LDH.

intercalated successfully without any structural alteration to the LDH layers.

The N_2 adsorption and desorption isotherms of LDH-PN-DC, LDH-PN-TC and LDH-PN-HC suggest that the LDH-PN materials display Type IV isotherms (Fig. 3d).[66] The specific surface areas of LDH-PN-DC, LDH-PN-TC and LDH-PN-HC are 37.5 m^2 g^{-1}, 22.0 m^2 g^{-1}, and 25.6 m^2 g^{-1}, respectively. Compared to Mg–Al–NO_3-LDH (74.6 m^2 g^{-1}) (Fig. S18†), the acid-intercalated LDHs possess a lower specific surface area due to the interlayer aggregation of three-dimensional cyclotriphosphazene carboxylate anions. These results indicate that the organic anions in cyclotriphosphazene can easily form dense structures with LDH.[47,51]

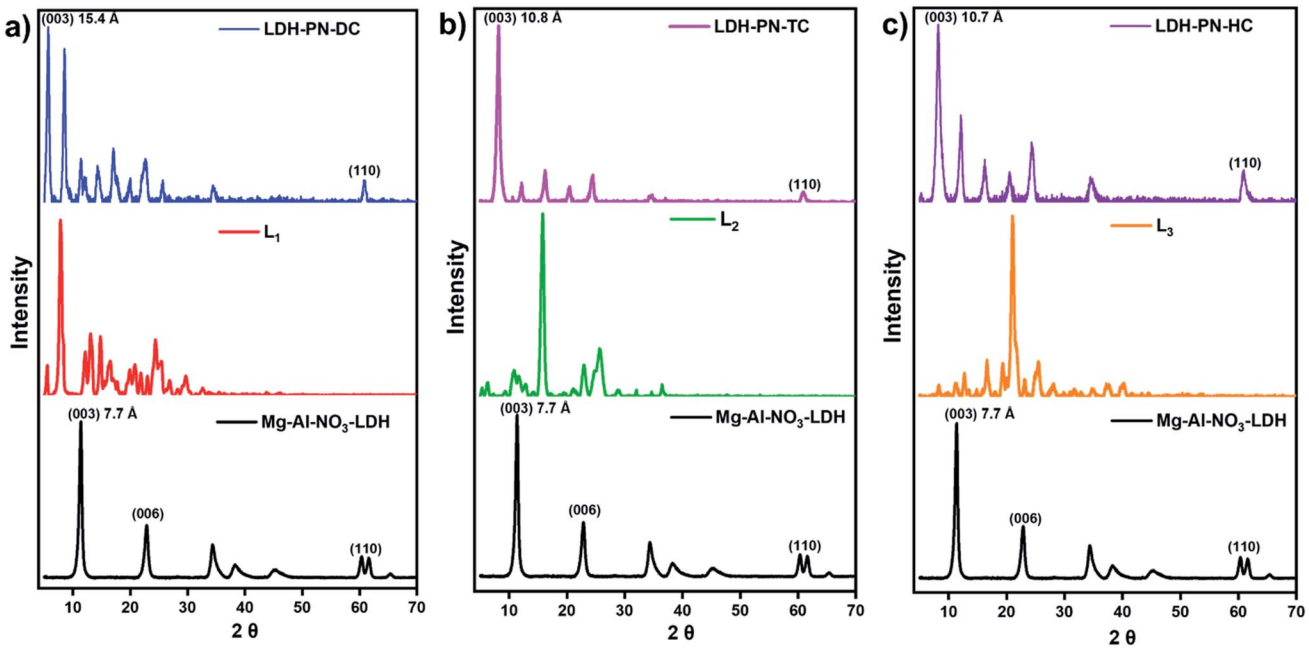

Fig. 1 Powder XRD patterns of (a) Mg–Al–NO_3-LDH, L_1 and LDH-PN-DC; (b) Mg–Al–NO_3-LDH, L_2 and LDH-PN-TC; (c) Mg–Al–NO_3-LDH, L_3 and LDH-PN-HC.

To examine the surface morphology, the HR-SEM images of Mg–Al–NO_3-LDH, LDH-PN-DC, LDH-PN-TC and LDH-PN-HC were captured and are shown in Fig. 4a. For Mg–Al–NO_3-LDH, thin flat platelets were found with irregular edges and arranged in all space directions, forming some aggregates. All the three LDH-PN materials showed more aggregation with non-uniform/irregular morphology compared to Mg–Al–NO_3-LDH. The guest anions are favourably stabilized on the basal face of the LDH structure during the LDH crystallization, causing the assembly with irregular morphology.[67] Therefore, this kind of structural assembly will be conducive to inhibiting heat transfer and thus remarkably improving the thermal stability of the LDH-PN materials. The elemental composition and distribution of the LDH-PN materials by HR-SEM are shown in Fig. 4b and S19.† The specific elements of magnesium, aluminum, phosphorus and nitrogen are well distributed, indicating that the LDH-PN materials are fairly homogeneous. The uniform distribution of the four main elements is significant for their flame retardant properties.

The elemental composition of the LDH-PN materials can be obtained from XPS analysis. The wide scan survey spectra and P 2p, N 1s, O 1s, Al 2p, and Mg 2p high-resolution spectra of LDH-PN-DC, LDH-PN-TC and LDH-PN-HC are presented in Fig. 5, S20 and S21,† respectively. The spectra for P 2p and N 1s of the LDH-PN materials reveal two major peaks at 134.0 ± 0.2 eV and 398.0 ± 0.1 eV, respectively, identifying the presence of P and N in the cyclotriphosphazene ring.[68–73] The spectra for O 1s of LDH-PN are divided into three peaks that indicate the presence

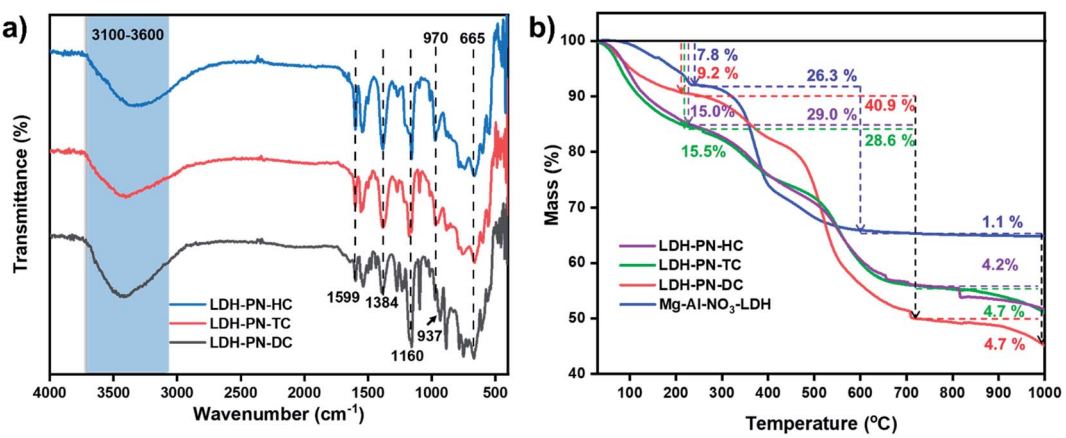

Fig. 2 (a) FT-IR spectra of the LDH-PN materials and (b) thermogravimetric analysis of the LDH-PN and Mg–Al–NO_3-LDH materials.

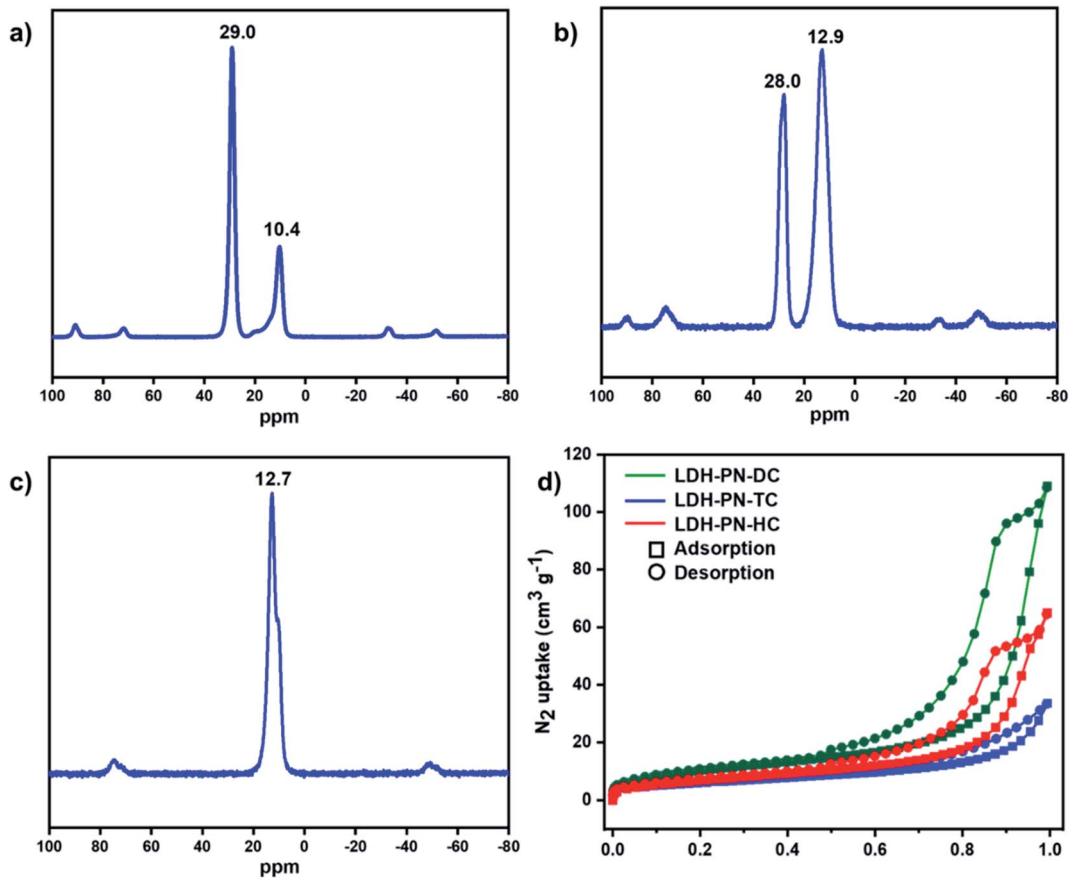

Fig. 3 Solid-state ^{31}P NMR spectra of (a) LDH-PN-DC, (b) LDH-PN-TC and (c) LDH-PN-HC; (d) N_2 adsorption and desorption isotherms for LDH-PN-DC, LDH-PN-TC and LDH-PN-HC.

of three different oxygen environments in the LDH-PN materials. The first peak at about 533.0 ± 0.4 eV is ascribed to the P–O–C bond in the intercalated anions, the second peak at 531.9 ± 0.1 eV is assigned to the C=O present in the carboxylate groups, and the final peak at about 530.7 ± 0.2 eV is attributed to the hydroxyl groups present in the hydroxide layers. Similarly,

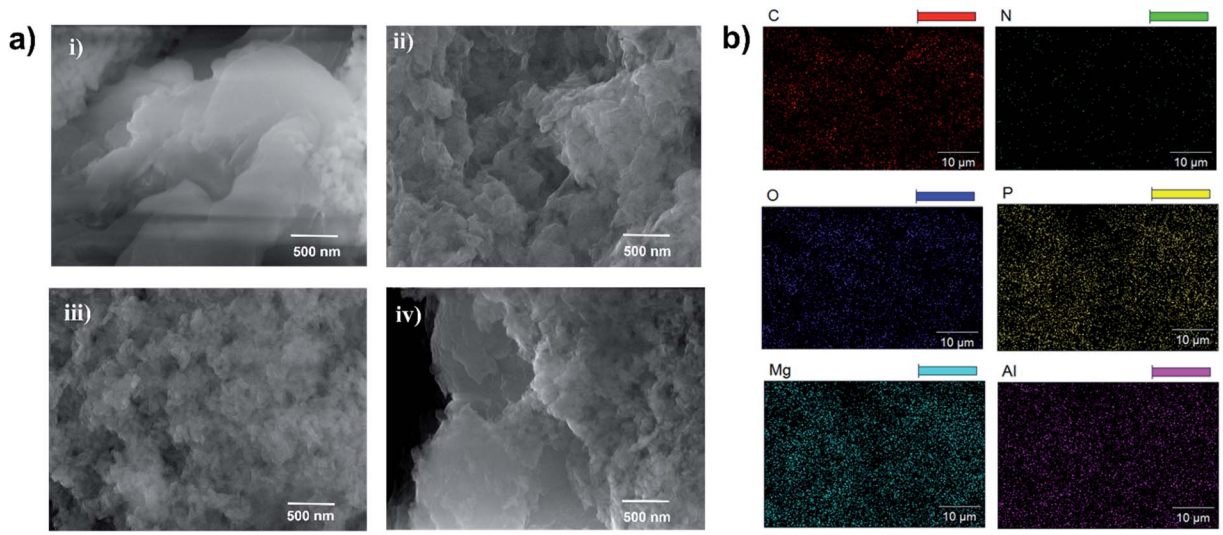

Fig. 4 (a) HR-SEM images of (i) Mg–Al–NO_3-LDH, (ii) LDH-PN-DC, (iii) LDH-PN-TC and (iv) LDH-PN-HC; (b) elemental mapping analysis of C, N, O, P, Mg, and Al in LDH-PN-DC.

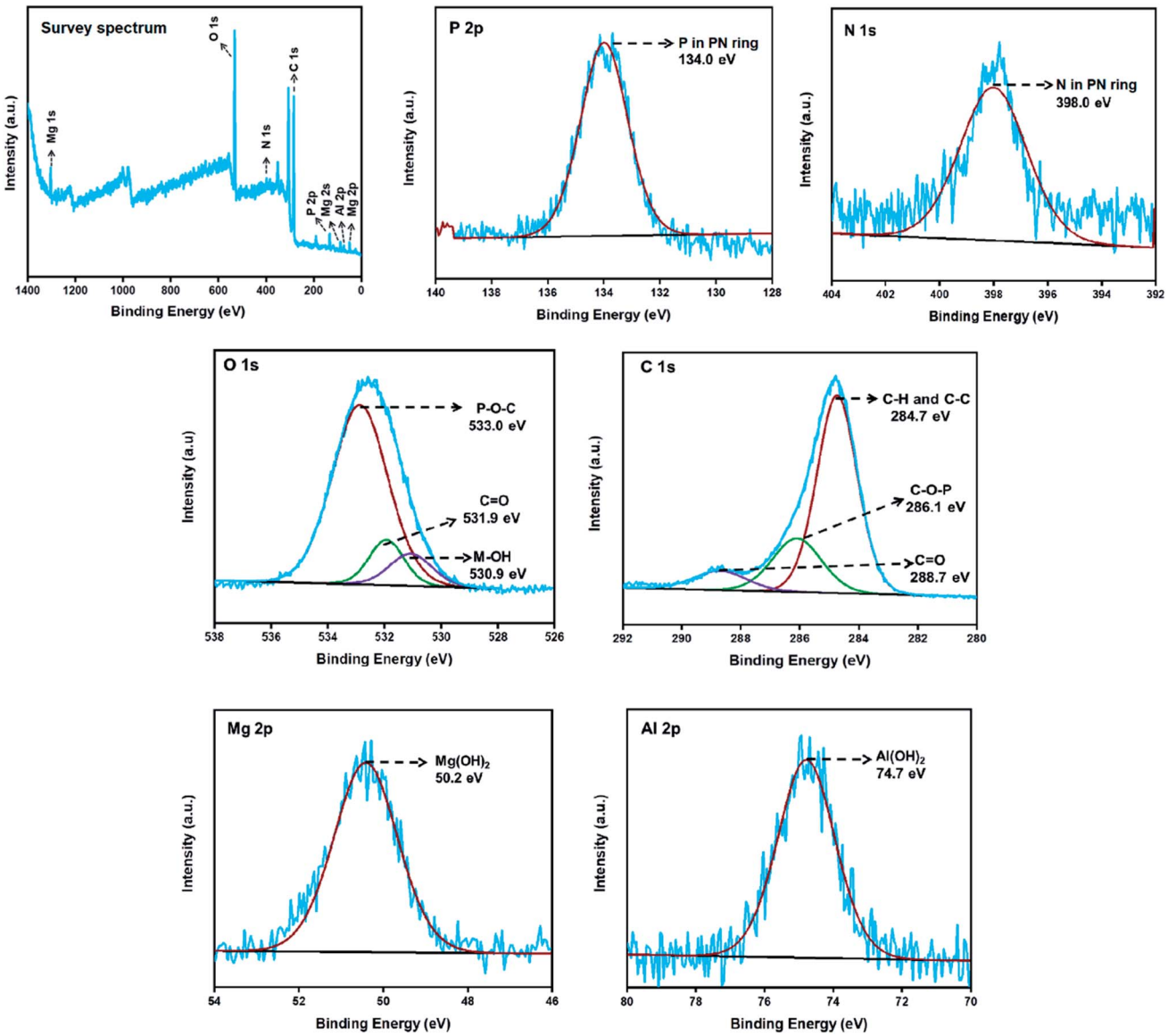

Fig. 5 XPS survey spectrum; P 2p, N 1s, O 1s, C 1s, Mg 2p and Al 2p high-resolution spectra of LDH-PN-DC.

the spectra for C 1s of the LDH-PN materials are distributed into three peaks that arise from the intercalated aromatic carboxylate anions. The peaks at 284.7 ± 0.3 eV, 286.1 ± 0.6 eV and 288.7 ± 0.2 eV are attributed to the C–C and C–H in the aromatic species, C–O–P in the PN species, and C═O in the carboxylate anions, respectively.[74,75] The peaks at 74.7 ± 0.1 eV for Al 2p and 50.2 ± 0 eV for Mg 2p are assigned to $Al(OH)_2$ and $Mg(OH)_2$, respectively, in the form of LDH layers in the LDH-PN materials.[76,77] These results indicate the successful intercalation of cyclotriphosphazene carboxylate anions into the LDH layers.

Flame retardant properties

Wood is commonly used for furniture and interior decoration materials owing to its abundance and outstanding mechanical properties. The flammable nature of wood is the main constraint on its use in interior environments, particularly in heavily populated zones. There is a high demand for state-of-the-art flame retardant technologies to protect wood from fire by coating it with highly flammable epoxy resin (EP).[45,78,79] Here, the EP/LDH-PN composites coated on the wood substrates exhibited flame retardancy to epoxy resin as well as protected the wood from flame. The assessment of flammability was carried out using a vertical burning test (UL-94 V) and the limiting oxygen index (LOI) test. The standard sizes of the wood substrates used for the UL 94 V test and LOI test were 130 × 13 × 5 mm^3 (ASTM D3801) and 150 × 7 × 3 mm^3 (ASTM D2863), respectively. In addition, the thickness of the epoxy resin and EP/LDH-PN composite-coated wood substrate was computed from cross-sectional microscopic images by measuring the thickness at 100 different points, and the value was 346.13 ± 16 μm (Fig. S22†). The epoxy resin-coated wood substrate and three EP/LDH-PN composite-coated wood substrates with different

weight percentages of LDH-PN materials from 5 to 20 wt% were used in the vertical burning test (UL-94 V). For example, EP/LDH-PN-DC-20 wt% denotes that the composite contains 20 wt% LDH-PN-DC.

The pure epoxy resin-coated wood substrate did not show any flame retardant properties in the UL-94 V tests. The entire length of the epoxy-coated wood substrate was completely burned after the second ignition time (30 seconds) in the UL-94 V test. The EP/LDH-PN-DC-20 wt% wood substrate did not capture the flame after the first ignition time, but during the second ignition time, it captured the flame and was completely burned after 30 seconds. Therefore, the EP/LDH-PN-DC-20 wt% wood substrates also failed the UL-94 V test (Fig. 6 and 7). However, EP/LDH-PN-TC-20 wt% and EP/LDH-PN-HC-20 wt% showed non-flammable behaviour and were classified with a V_0 rating in the vertical burning test (Fig. 6 and 7). Both samples did not capture the flame during the first and the second ignition times, which proves the importance of the nature of cyclotriphosphazene carboxylate anions within the LDH layers. The cyclotriphosphazene dicarboxylate anions ($\mathbf{L_1}$) in LDH-PN-DC, tetracarboxylate anions ($\mathbf{L_2}$) in LDH-PN-TC and hexacarboxylate anions ($\mathbf{L_3}$) in LDH-PN-HC consist of two spiro groups with two carboxylate binding sites, one spiro group with four carboxylate binding sites and only six carboxylate binding sites, respectively. Thus, the smaller number of spiro groups and more binding sites assist the effective dispersion of epoxy resin in the LDH layers, resulting in the superior flame retardant properties of the EP/LDH-PN-TC-20 wt% and EP/LDH-PN-HC-20 wt% composites. In other words, the more spiro groups and smaller number of binding sites inhibit the dispersion of epoxy resin in the LDH layers, leading to the separate aggregation of LDH-PN-DC in the EP/LDH-PN-DC-20 wt% composite, which failed in terms of flame retardant properties. Furthermore, the flame retardant properties of the EP/Mg–Al–NO_3-LDH-20 wt%, EP/$\mathbf{L_1}$-20 wt% and EP/$\mathbf{L_3}$-20 wt%-coated wooden samples were tested in the UL-94 V test and all these samples failed by demonstrating their highly flammable behaviour (Fig. S23†). Hence, compared to EP/Mg–Al–NO_3-LDH, EP/$\mathbf{L_1}$ and EP/$\mathbf{L_3}$, the flame retardant properties of the EP/LDH-PN composites are improved due to the synergistic flame retardant effect of the combination of LDH and cyclotriphosphazene in the epoxy resins.

The limiting oxygen index (LOI) is an important parameter for evaluating the flame retardancy of samples, which measures the minimum oxygen concentration of a flowing gas comprising oxygen and nitrogen required to support downward flame combustion. Epoxy coated on the wood substrate was highly flammable and had an LOI value of 23.2 vol%. However, EP/LDH-PN-DC coated on the wood substrate showed a lower LOI value of 22.1 vol% than the epoxy wood substrate. Compared with those of the epoxy and EP/LDH-PN-DC-coated wood substrates, the LOI values of the EP/LDH-PN-TC and EP/LDH-PN-HC-coated wood substrates increased to 27.7 vol% and 29 vol%, respectively. Therefore, the result of the LOI test indicates that both the EP/LDH-PN-TC and EP/LDH-PN-HC composites impart excellent flame retardancy to epoxy resin on wood substrates, which demonstrates the significant role of the spiro groups and binding sites present in cyclotriphosphazene.

Based on the above analysis, we proposed a mechanism for the flame retardancy of the EP/LDH-PN composites on the wood substrate, as shown in Scheme 2.

During the combustion process, the decomposition of cyclotriphosphazene and the LDH layers produces degraded PN rings with the emission of non-flammable gases (CO_2 and N_2) and metal oxides with water vapour, respectively.[32,80,81] This

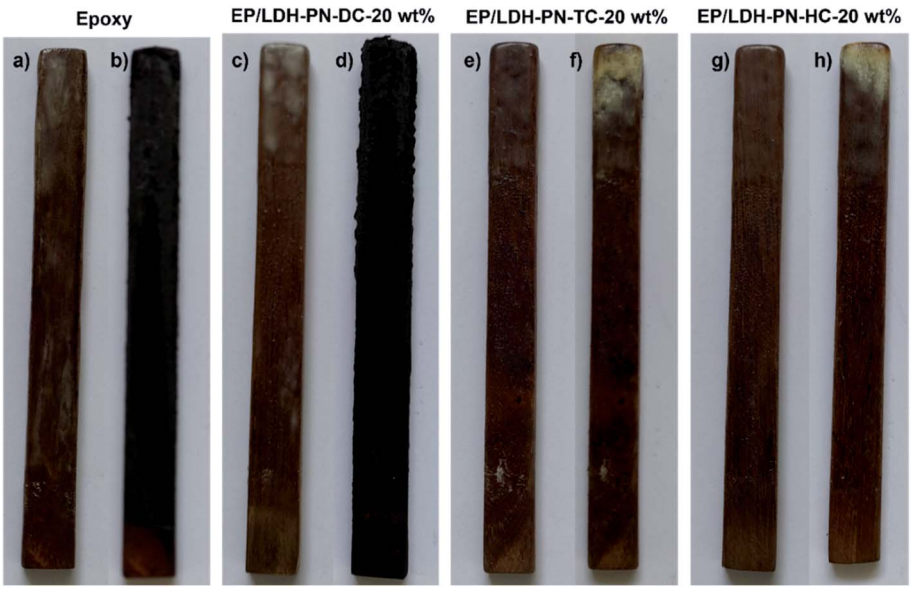

Fig. 6 Digital photos before (a, c, e and g) and after (b, d, f and h) the UL-94 vertical burning tests of the epoxy and EP/LDH-PN composite-coated wood substrates.

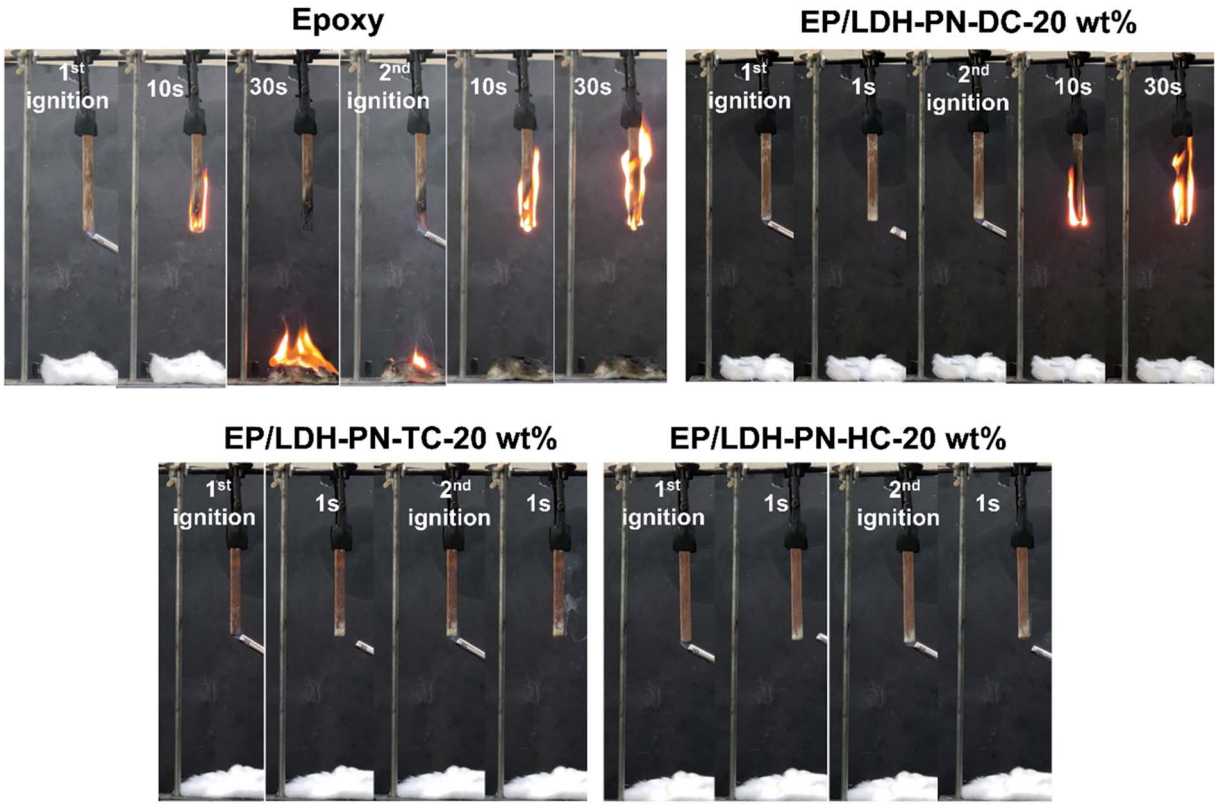

Fig. 7 Digital photos of the pure epoxy resin, EP/LDH-PN-DC-20 wt%, EP/LDH-PN-TC-20 wt%, and EP/LDH-PN-HC-20 wt% composite-coated wood substrates during the UL-94 V vertical burning process.

synergistic effect of cyclotriphosphazene and LDH in the EP/LDH-PN composite leads to the formation of a white layer of non-volatile protective film on the surface of the wood substrate. Thus, the non-volatile protective film insulates the wood substrate from the air, absorbs the heat, and increases the ignition time, which prevents oxygen supply during the combustion process.

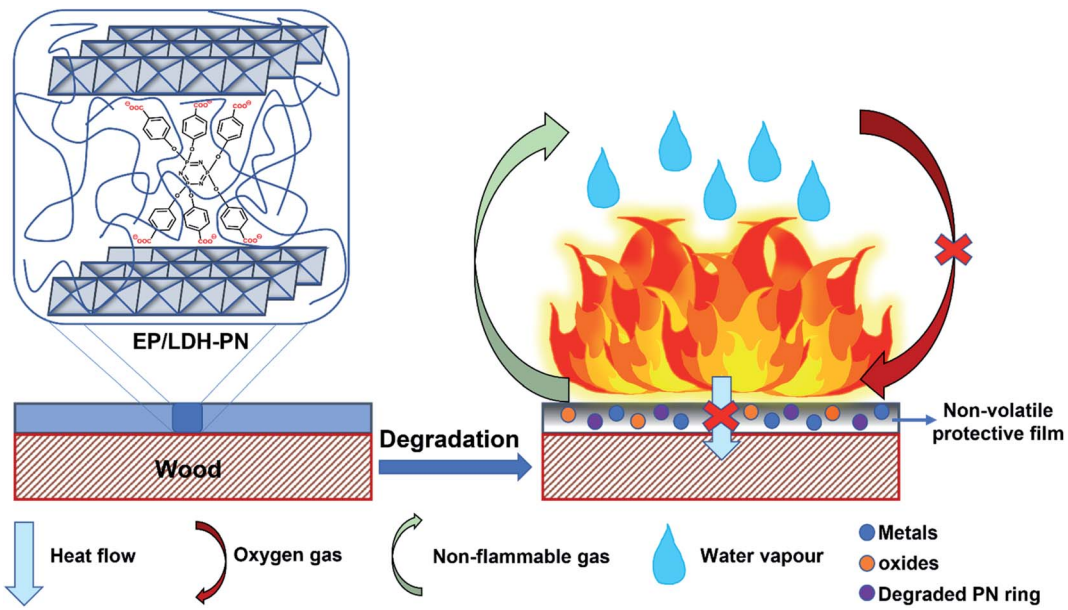

Scheme 2 Schematic illustration of the flaming of the EP/LDH-PN composite-coated wood substrate.

Conclusion

A series of environmentally friendly LDHs have been prepared with different cyclotriphosphazene carboxylate anions as intercalating guest molecules and their flame retardant properties have been examined. Their powder XRD patterns demonstrate that the interlayer distance of all the LDH-PN materials increases upon the intercalation reactions of LDH with cyclotriphosphazene carboxylate anions compared with that of pristine Mg–Al–NO_3-LDH, and the diffraction peak at $2\theta \simeq 60.8^\circ$ in the LDH-PN materials confirms the formation of the layered structures. From TGA, the first and second weight loss percentages for LDH-PN-TC and LDH-PN-HC are found to be almost the same but different from that of the LDH-PN-DC material due to the number of binding sites of the cyclotriphosphazene carboxylate anions. Fourier transform infrared spectroscopy and X-ray photoelectron spectroscopy further confirmed the presence of cyclotriphosphazene carboxylate anions in the LDH layers. Flame retardant tests (UL-94 V and LOI tests) were performed using epoxy resin with varying weight percentages of LDH-PN materials (5–20 wt%) coated on wood substrates. EP/LDH-PN-TC-20 wt% and EP/LDH-PN-HC-20 wt% passed the UL-94 V test with a V_0 rating and showed higher LOI values, which demonstrated that these materials do not show burning properties and completely protect the wood substrate from the flame. However, the EP/LDH-PN-DC samples with different ratios of LDH-PN-DC from 5% to 20 wt% showed no self-extinguishing properties and burned to completion in the UL-94 test and showed a lower LOI value of 22.1 vol%. Hence, the incorporation of either LDH-PN-HC or LDH-PN-TC into the epoxy resin significantly improves the flame retardant properties compared to that in LDH-PN-DC because of their cyclotriphosphazene structure with more binding carboxylate sites and less or no bulky spiro groups that result in the good dispersion of LDH-PN-HC or LDH-PN-TC in the polymer matrix, and the unique combination of LDH and cyclotriphosphazene resulted in a synergistic flame retardant effect. Therefore, this work provides a feasible strategy to design sustainable halogen-free flame retardant materials to resolve the common issues related to environmental safety and human health.

Author contributions

Conceived and designed the experiments: V. J. and S. S.; performed the experiments: V. J.; measured and analyzed the spectroscopic data: V. J. and S. S.; wrote the paper: S. S. and V. J.

Conflicts of interest

There are no conflicts to declare.

Acknowledgements

SS gratefully acknowledges the Science and Engineering Research Board, Department of Science and Technology, Government of India, for providing financial aid under the core research grant (CRG/2019/001254). We thank DST-FIST for the Department of Chemistry and Nanotechnology Research Centre, SRM IST for the PXRD and XPS facilities.

References

1 (*a*) J. Troitzsch, Flame retardants, *Kunstst. Int.*, 1996, **86**, 960–964; (*b*) K. Kampke-Thiel, D. Lenoir, A. Kettrup, E. Herdtweck, D. Gleich and W. R. Thiel, Isolation, characterization, and toxicological aspects of volatile organophosphorus compounds from the combustion of flame-retarded epoxy resins with phosphonate substructures, *Chem.–Eur. J.*, 1998, **4**, 1581–1586; (*c*) S. Zhang, Y. Jiang, Y. Sun, J. Sun, B. Xu, H. Li and X. Gu, Preparation of flame retardant and conductive epoxy resin materials by incorporating functionalized multi-walled carbon nanotubes and graphite sheets, *Polym. Adv. Technol.*, 2021, **32**, 2093–2101.

2 (*a*) M. Venier, A. Salamova and R. A. Hites, Halogenated flame retardants in the great lakes environment, *Acc. Chem. Res.*, 2015, **48**, 1853–1861; (*b*) H. Thoma, S. Rist, G. Hauschulz and O. Hutzinger, Polybrominated dibenzodioxins (PBrDD) and dibenzofurans (PBrDF) in some flame retardant preparations, *Chemosphere*, 1986, **15**, 2111–2113.

3 (*a*) D. Lenoir and K. Kampke-Thiel, Formation of polybrominated dibenzodioxins and furans in laboratory combustion processes of brominated flame retardants, in *Fire and Polymers*, Ed., G. Nelson, ACS Series No. 599, 1995, 2, pp. 377–392; (*b*) C. A. De Wit, An Overview of brominated flame retardants in the environment, *Chemosphere*, 2002, **46**, 583–624.

4 (*a*) L. S. Birnbaum and D. F. Staskal, Brominated flame retardants: Cause for concern?, *Environ. Health Perspect.*, 2004, **112**, 9–17; (*b*) Y.-L. Wei, L.-J. Bao, C.-C. Wu and E. Y. Zeng, Characterization of anthropogenic impacts in a large urban center by examining the spatial distribution of halogenated flame retardants, *Environ. Pollut.*, 2016, **215**, 187–194.

5 S. N. Zhou, A. Buchar, S. Siddique, L. Takser, N. Abdelouahab and J. Zhu, Measurements of selected brominated flame retardants in nursing woman: Implications for human exposure, *Environ. Sci. Technol.*, 2014, **48**, 8873–8880.

6 (*a*) K. Ham, H. Jin, R. Al-Raoush, X. Xie, C. S. Willson, G. R. Byerly, L. S. Simeral, M. L. Rivers, R. L. Kurtz and L. G. Butler, Three-dimensional chemical analysis with synchrotron tomography at multiple x-ray energies: Brominated aromatic flame Retardant and antimony oxide in polystyrene, *Chem. Mater.*, 2004, **16**, 4032–4042; (*b*) B. B. Marosfoi, S. Garas and B. Bodzayl, Flame retardancy study on magnesium hydroxide associated with clays of different morphology in polypropylene matrix, *Polym. Adv. Technol.*, 2008, **19**, 693–700; (*c*) N. Wang, Y. Fu, Y. Liu, H. Yu and Y. Liu, Synthesis of aluminum hydroxide thin coating and its influence on the thermomechanical and fire-resistant properties of wood, *Holzforschung*, 2014, **68**, 781–789.

7 (*a*) Y. Zhao, F. Li, R. Zhang, D. G. Evans and X. Duan, Preparation of layered double-hydroxide nanomaterials with a uniform crystallite size using a new method involving separate nucleation and aging steps, *Chem. Mater.*, 2002, **14**, 4286–4291; (*b*) Q. Wang and D. O'Hare, Recent advances in the synthesis and application of layered double hydroxide (LDH) nanosheets, *Chem. Rev.*, 2012, **112**, 4124–4155; (*c*) J.-Z. Du, L. Jin, H.-Y. Zeng, X.-k. Shi, E.-g. Zhou, B. Feng and X. Sheng, Flame retardancy of organic-anion-intercalated layered double hydroxides in ethylene vinyl acetate copolymer, *Appl. Clay Sci.*, 2019, **180**, 105193.

8 (*a*) A. I. Khan and D. O'Hare, Intercalation chemistry of layered double hydroxides: recent developments and applications, *J. Mater. Chem.*, 2002, **12**, 3191–3198; (*b*) Y. Liu, Y. Gao, Q. Wang and W. Lin, The synergistic effect of layered double hydroxides with other flame retardant additives for polymer nanomaterials: a critical review, *Dalton Trans.*, 2018, **47**, 14827–14840; (*c*) L. Jin, H.-Y. Zeng, J.-Z. Du and S. Xu, Intercalation of organic and inorganic anions into layered double hydroxides for polymer flame retardancy, *Appl. Clay Sci.*, 2020, **187**, 105481.

9 (*a*) V. Rives, *Layered double hydroxides: present and future*, Nova Publishers, 2001; (*b*) J. Yu, Q. Wang, D. O'Hare and L. Sun, Preparation of two dimensional layered double hydroxide nanosheets and their applications, *Chem. Soc. Rev.*, 2017, **46**, 5950–5974; (*c*) K. Ruengkajorn, C. M. R. Wright, N. H. Rees, J.-C. Buffet and D. O'Hare, Aqueous immiscible layered double hydroxides – AIM-LDHs, *Mater. Chem. Front.*, 2018, **2**, 2277–2285.

10 (*a*) V. Rives, Characterisation of layered double hydroxides and their decomposition products, *Mater. Chem. Phys.*, 2002, **75**, 19–25; (*b*) N. O'Toole, C. Lecourt, Y. Suffren, F. Toche, R. Chiriac, N. Gilon, F. Bessueille, A. Brioude, E. Jeanneau, D. Luneau and C. Desroches, Intercalation of a manganese (II)-thiacalixarene luminescent complex in layered double hydroxides: synthesis and photophysical characterization, *New J. Chem.*, 2021, **45**, 343–350.

11 (*a*) Z. Matusinovic, J. Feng and C. A. Wilkie, The role of dispersion of LDH in fire retardancy: The effect of different divalent metals in benzoic acid modified LDH on dispersion and fire retardant properties of polystyrene- and poly(methyl-methacrylate)-LDH-B nanomaterials, *Polym. Degrad. Stab.*, 2013, **98**, 1515–1525; (*b*) Q. Zhang, Y. Guo, A. A. Marek, V. Verney, F. Leroux, P. Tang, D. Li and Y. Feng, Design, fabrication and anti-aging behavior of a multifunctional inorganic–organic hybrid stabilizer derived from co-intercalated layered double hydroxides for polypropylene, *Inorg. Chem. Front.*, 2019, **6**, 3350.

12 (*a*) N. Nhlapo, T. Motumi, E. Landman, S. M. C. Verryn and W. W. Focke, Surfactant-assisted fatty acid intercalation of layered double hydroxides, *J. Mater. Sci.*, 2008, **43**, 1033–1043; (*b*) N. Iyi, Y. Ebina and T. Sasaki, Synthesis and characterization of water-swellable LDH (layered double hydroxide) hybrids containing sulfonate-type intercalant, *J. Mater. Chem.*, 2011, **21**, 8085–8095; (*c*) H. Zhang, Z. P. Xu, G. Q. Lu and S. C. Smith, Intercalation of sulfonate into layered double hydroxide: Comparison of simulation with experiment, *J. Phys. Chem. C*, 2009, **113**, 559–566; (*d*) G. R. Williams, N. H. Rees and D. O'Hare, Incorporation of phosphorus oxyacids into layered double hydroxides, *Solid State Sci.*, 2009, **11**, 1229–1238.

13 (*a*) N. Iyi, Y. Ebina and T. Sasaki, Water-swellable MgAl−LDH (Layered Double Hydroxide) hybrids: Synthesis, Characterization, and Film preparation, *Langmuir*, 2008, **24**, 5591–5598; (*b*) J. H. Lee, S. W. Rhee and D.-Y. Jung, Selective layer reaction of layer-by-layer assembled layered double-hydroxide nanocrystals, *J. Am. Chem. Soc.*, 2007, **129**, 3522–3523.

14 (*a*) C. Nyambo, P. Songtipya, E. Manias, M. M. Jimenez-Gasco and C. A. Wilkie, Effect of MgAl-layered double hydroxide exchanged with linear alkyl carboxylates on fire-retardancy of PMMA and PS, *J. Mater. Chem.*, 2008, **18**, 4827–4838; (*b*) C. Manzi-Nshuti, J. M. Hossenlopp and C. A. Wilkie, Comparative study on the flammability of polyethylene modified with commercial fire retardants and a zinc aluminum oleate layered double hydroxide, *Polym. Degrad. Stab.*, 2009, **94**, 782–788; (*c*) N.-J. Kang, D.-Y. Wang, B. Kutlu, P.-C. Zhao, A. Leuteritz, U. Wagenknecht and G. Heinrich, A new approach to reducing the flammability of layered double hydroxide (LDH)-based polymer materials: Preparation and characterization of dye structure-intercalated LDH and its effect on the flammability of polypropylene-grafted maleic anhydride/d-LDH materials, *ACS Appl. Mater. Interfaces*, 2013, **5**, 8991–8997.

15 (*a*) F. R. Costa, U. Wagenknecht and G. Heinrich, LDPE/Mg–Al layered double hydroxide nanomaterial: Thermal and flammability properties, *Polym. Degrad. Stab.*, 2007, **92**, 1813–1823; (*b*) D.-Y. Wang, A. Leuteritz, Y.-Z. Wang, U. Wagenknecht and G. Heinrich, Preparation and burning behaviors of flame retarding biodegradable poly(lactic acid) nanomaterial based on zinc aluminum layered double hydroxide, *Polym. Degrad. Stab.*, 2010, **95**, 2474–2480; (*c*) B. Sahu and G. Pugazhenthi, Properties of polystyrene/organically modified layered double hydroxide nanomaterials synthesized by solvent blending method, *J. Appl. Polym. Sci.*, 2011, **120**, 2485–2495.

16 Z. Zhang, J. Qin, W. Zhang, Y.-T. Pan, D.-Y. Wang and R. Yang, Synthesis of a novel dual layered double hydroxide hybrid nanomaterial and its application in epoxy nanomaterials, *Chem. Eng. J.*, 2020, **381**, 122777.

17 M. Zammarano, M. Franceschi, S. Bellayer, J. W. Gilman and S. Meriani, Preparation and flame resistance properties of revolutionary self-extinguishing epoxy nanomaterials based on layered double hydroxides, *Polymer*, 2005, **46**, 9314–9328.

18 L. Shi, D. Li, J. Wang, S. Li, D. G. Evans and X. Duan, Synthesis, flame-retardant and smoke-suppressant properties of a borate-intercalated layered double hydroxide, *Clays Clay Miner.*, 2005, **53**, 294–300.

19 L. Ye and B. Qu, Flammability characteristics and flame retardant mechanism of phosphate-intercalated hydrotalcite in halogen-free flame retardant EVA blends, *Polym. Degrad. Stab.*, 2008, **93**, 918–924.

20 (*a*) V. Chandrasekhar and S. Nagendran, Phosphazenes as scaffolds for the construction of multi-site coordination ligands, *Chem. Soc. Rev.*, 2001, **30**, 193–203; (*b*) V. Chandrasekhar, P. Thilagar and B. Murugesa Pandian, Cyclophosphazene-based multi-site coordination ligands, *Coord. Chem. Rev.*, 2007, **251**, 1045–1074; (*c*) A. Uslu and S. Yeşilot, Recent advances in the supramolecular assembly of cyclophosphazene derivatives, *Dalton Trans.*, 2021, **50**, 2324–2341; (*d*) V. Jeevananthan, S. A. G. Thangavelu, P. Loganathan and S. Shanmugan, Multisite coordination ligands on cyclotriphosphazene core for the assembly of metal clusters and porous coordination polymers, *ChemistrySelect*, 2021, **6**, 1478–1507.

21 (*a*) S. Beşli, C. Mutlu Balcı, S. Doğan and C. W. Allen, Regiochemical control in the substitution reactions of cyclotriphosphazene derivatives with secondary amines, *Inorg. Chem.*, 2018, **57**, 12066–12077; (*b*) D. Bai, F. Chen, D. Jiang and Y. He, A rare Pb9 cluster-organic framework constructed from a flexible cyclotriphosphazene-functionalized hexacarboxylate exhibiting selective gas separation, *Inorg. Chem. Front.*, 2017, **4**, 1501–1508; (*c*) J. Chen, L. Wang, Y. Fan, Y. Yang, M. Xu and X. Shi, Synthesis and anticancer activity of cyclotriphosphazenes functionalized with 4-methyl-7-hydroxycoumarin, *New J. Chem.*, 2019, **43**, 18316–18321.

22 (*a*) J. Sun, Z. Yu, X. Wang and D. Wu, Synthesis and performance of cyclomatrix polyphosphazene derived from trispiro-cyclotriphosphazene as a halogen-Free nonflammable material, *ACS Sustainable Chem. Eng.*, 2014, **2**, 231–238; (*b*) K. Krishnadevi and V. Selvaraj, Development of halogen-free flame retardant phosphazene and rice husk ash incorporated benzoxazine blended epoxy materials for microelectronic applications, *New J. Chem.*, 2015, **39**, 6555–6567; (*c*) H. Lim and J. Y. Chang, Thermally stable and flame retardant low dielectric polymers based on cyclotriphosphazenes, *J. Mater. Chem.*, 2010, **20**, 749–754.

23 (*a*) P. Jiang, X. Gu, S. Zhang, S. Wu, Q. Zhao and Z. Hu, Synthesis, characterization, and utilization of a novel phosphorus/nitrogen-containing flame retardant, *Ind. Eng. Chem. Res.*, 2015, **54**, 2974–2982; (*b*) M. M. Velencoso, A. Battig, J. C. Markwart, B. Schartel and F. R. Wurm, Molecular firefighting—how modern phosphorus chemistry can help solve the challenge of flame retardancy, *Angew. Chem., Int. Ed.*, 2018, **57**, 10450–10467; (*c*) H. Wang, X. Du, S. Wang, Z. Du, H. Wang and X. Cheng, Improving the flame retardancy of waterborne polyurethanes based on the synergistic effect of P–N flame retardants and a Schiff base, *RSC Adv.*, 2020, **10**, 12078–12088.

24 (*a*) O. Dagdag, A. E. Bachiri, O. Hamed, R. Haldhar, C. Verma, E. Ebenso and M. E. Gouri, Dendrimeric epoxy resins based on hexachlorocyclotriphosphazene as a reactive flame retardant polymeric materials: A review, *J. Inorg. Organomet. Polym. Mater.*, 2021, **31**, 3240–3261; (*b*) B. Edwards, S. Rudolf, P. Hauser and A. El-Shafei, Preparation, polymerization, and performance evaluation of halogen-free radiation curable flame retardant monomers for cotton substrates, *Ind. Eng. Chem. Res.*, 2015, **54**, 577–584.

25 Y. Chen, X. Wu and L. Qian, Flame-retardant behavior and protective layer effect of phosphazene-triazine bi-group flame retardant on polycarbonate, *J. Appl. Polym. Sci.*, 2020, **137**, 49523.

26 J. Xu, Z. He, W. Wu, H. Ma, J. Xie, H. Qu and Y. Jiao, Study of thermal properties of flame retardant epoxy resin treated with hexakis[p-(hydroxymethyl)phenoxy] cyclotriphosphazene, *J. Therm. Anal. Calorim.*, 2013, **114**, 1341–1350.

27 C. Zhang, X. Guo, S. Ma, Y. Zheng, J. Xu and H. Ma, Synthesis of a novel branched cyclophosphazene-PEPA flame retardant and its application on polypropylene, *J. Therm. Anal. Calorim.*, 2019, **137**, 33–42.

28 M. Xu, K. Ma, D. Jiang, J. Zhang, M. Zhao, X. Guo, Q. Shao, E. Wujcik, B. Li and Z. Guo, Hexa-[4-(glycidyloxycarbonyl) phenoxy]cyclotriphosphazene chain extender for preparing high-performance flame retardant polyamide 6 materials, *Polymer*, 2018, **146**, 63–72.

29 Y. Yang, W. Kong and X. Cai, Two phosphorous-containing flame retardant form a novel intumescent flame-retardant system with polycarbonate, *Polym. Degrad. Stab.*, 2016, **134**, 136–143.

30 J. Köhler, S. Kühl, H. Keul, M. Möller and A. Pich, Synthesis and characterization of polyamine-based cyclophosphazene hybrid microspheres, *J. Polym. Sci., Part A: Polym. Chem.*, 2014, **52**, 527–536.

31 Y. Bai, X. Wang and D. Wu, Novel cyclolinear cyclotriphosphazene-linked epoxy resin for halogen-free fire resistance: Synthesis, characterization, and flammability characteristics, *Ind. Eng. Chem. Res.*, 2012, **51**, 15064–15074.

32 J. Sun, X. Wang and D. Wu, Novel spirocyclic phosphazene-based epoxy resin for halogen-free fire resistance: Synthesis, curing behaviors, and flammability characteristics, *ACS Appl. Mater. Interfaces*, 2012, **4**, 4047–4061.

33 Y. Fang, X. Du, S. Yang, H. Wang, X. Cheng and Z. Du, Sustainable and tough polyurethane films with self-healability and flame retardance enabled by reversible chemistry and cyclotriphosphazene, *Polym. Chem.*, 2019, **10**, 4142–4153.

34 D. Mathew, C. P. R. Nair and K. N. Ninan, Phosphazene–triazine cyclomatrix network polymers: some aspects of synthesis, thermal- and flame-retardant characteristics, *Polym. Int.*, 2000, **49**, 48–56.

35 G.-R. Xu, M.-J. Xu and B. Li, Synthesis and characterization of a novel epoxy resin based on cyclotriphosphazene and its thermal degradation and flammability performance, *Polym. Degrad. Stab.*, 2014, **109**, 240–248.

36 Y. Huang, T. Ma, Q. Wang and C. Guo, Synthesis of biobased flame-retardant carboxylic acid curing agent and application in wood surface coating, *ACS Sustainable Chem. Eng.*, 2019, **7**, 14727–14738.

37 J.-w. Gu, G.-c. Zhang, S.-l. Dong, Q.-y. Zhang and J. Kong, Study on preparation and fire-retardant mechanism

analysis of intumescent flame-retardant coatings, *Surf. Coat. Technol.*, 2007, **201**, 7835–7841.

38 G. F. Levchik, Y. V. Grigoriev, A. I. Balabanovich, S. V. Levchik and M. Klatt, Phosphorus–nitrogen containing fire retardants for poly(butylene terephthalate), *Polym. Int.*, 2000, **49**, 1095–1100.

39 C. W. Allen, The use of phosphazenes as fire resistant materials, *J. Fire Sci.*, 1993, **11**, 320–328.

40 (*a*) X. Shan, L. Song, W. Xing, Y. Hu and S. Lo, Effect of nickel-containing layered double hydroxides and cyclophosphazene compound on the thermal stability and flame retardancy of poly(lactic acid), *Ind. Eng. Chem. Res.*, 2012, **51**, 13037–13045; (*b*) X. Zhou, X. Mu, W. Cai, J. Wang, F. Chu, Z. Xu and Y. Hu, Design of hierarchical NiCo-LDH@PZS hollow dodecahedron architecture and application in high-performance epoxy resin with excellent fire safety, *ACS Appl. Mater. Interfaces*, 2019, **11**, 41736–41749.

41 G. A. Carriedo, L. Fernández-Catuxo, F. J. García Alonso, P. Gómez-Elipe and P. A. González, Preparation of a new type of phosphazene high polymers containing 2,2'-dioxybiphenyl groups, *Macromolecules*, 1996, **29**, 5320–5325.

42 G. A. Carriedo, F. J. Garcia-Alonso, J. L. García-Alvarez, G. C. Pappalardo, F. Punzo and P. Rossi, Stereoisomer discrimination through π-stacking interactions in spirocyclic phosphazenes bearing 2, 2′-Dioxybiphenyl units, *Eur. J. Inorg. Chem.*, 2003, **2003**, 2413–2418.

43 B. Li, X. Chen, F. Yu, W. Yu, T. Zhang and D. Sun, Luminescent response of one anionic metal–organic framework based on novel octa-nuclear zinc cluster to exchanged cations, *Cryst. Growth Des.*, 2014, **14**, 410–413.

44 C. M. Becker, A. D. Gabbardo, F. Wypych and S. C. Amico, Mechanical and flame-retardant properties of epoxy/Mg–Al LDH materials, *Materials*, 2011, **42**, 196–202.

45 A. R. Sethurajaperumal, A. Manohar, A. Banerjee, E. Varrla, H. Wang and K. Ostrikov, Thermally-insulating vermiculite nanosheets-epoxy nanomaterial paint as fire-resistant wood coating, *Nanoscale Adv.*, 2021, **3**, 4235–4243.

46 H. N. Tran, C.-C. Lin and H.-P. Chao, Amino acids-intercalated Mg/Al layered double hydroxides as dual-electronic adsorbent for effective removal of cationic and oxyanionic metal ions, *Sep. Purif. Technol.*, 2018, **192**, 36–45.

47 M. Bouraada, M. S. Ouali and L. C. de Ménorval, Dodecylsulfate and dodecybenzenesulfonate intercalated hydrotalcites as adsorbent materials for the removal of BBR acid dye from aqueous solutions, *J. Saudi Chem. Soc.*, 2016, **20**, 397–404.

48 A. N. Ay, H. Akar, A. Zaulet, C. Viñas, F. Teixidor and B. Zumreoglu-Karan, Carborane-layered double hydroxide nanohybrids for potential targeted- and magnetically targeted-BNCT applications, *Dalton Trans.*, 2017, **46**, 3303–3310.

49 S. Marappa, S. Radha and P. V. Kamath, Nitrate-intercalated layered double hydroxide-structure model, order, and disorder, *Eur. J. Inorg. Chem.*, 2013, **2013**, 2122–2128.

50 F. Millange, R. I. Walton and D. O'Hare, Time-resolved *in situ* X-ray diffraction study of the liquid-phase reconstruction of Mg–Al–carbonate hydrotalcite-like compounds, *J. Mater. Chem.*, 2000, **10**, 1713–1720.

51 H. N. Tran, C.-C. Lin, S. H. Woo and H.-P. Chao, Efficient removal of copper and lead by Mg/Al layered double hydroxides intercalated with organic acid anions: Adsorption kinetics, isotherms, and thermodynamics, *Appl. Clay Sci.*, 2018, **154**, 17–27.

52 J. Cai, H.-M. Heng, X.-P. Hu, Q.-K. Xu and F. Miao, A facile method for the preparation of novel fire-retardant layered double hydroxide and its application as nanofiller in UP, *Polym. Degrad. Stab.*, 2016, **126**, 47–57.

53 Q. Yuan, M. Wei, D. G. Evans and X. Duan, Preparation and investigation of thermolysis of l-aspartic acid-intercalated layered double hydroxide, *J. Phys. Chem. B*, 2004, **108**, 12381–12387.

54 (*a*) Z. P. Xu and H. C. Zeng, Abrupt structural transformation in hydrotalcite-like compounds $Mg_{1-x}Al_x(OH)_2(NO_3)_x \cdot nH_2O$ as a continuous function of nitrate anions, *J. Phys. Chem. B*, 2001, **105**, 1743–1749; (*b*) S. Mallakpour and M. Dinari, Intercalation of amino acid containing chiral dicarboxylic acid between Mg–Al layered double hydroxide, *J. Therm. Anal. Calorim.*, 2015, **119**, 1123–1130.

55 (*a*) S. Yang, J. Wang, S. Huo, J. Wang and Y. Tang, Synthesis of a phosphorus/nitrogen-containing compound based on maleimide and cyclotriphosphazene and its flame-retardant mechanism on epoxy resin, *Polym. Degrad. Stab.*, 2016, **126**, 9–16; (*b*) C. Y. Yuan, S. Y. Chen, C. H. Tsai, Y. S. Chiu and Y. W. Chen-Yang, Thermally stable and flame-retardant aromatic phosphate and cyclotriphosphazene-containing polyurethanes: synthesis and properties, *Polym. Adv. Technol.*, 2005, **16**, 393–399.

56 (*a*) M. Wei, M. Pu, J. Guo, J. Han, F. Li, J. He, D. G. Evans and X. Duan, Intercalation of l-dopa into layered double hydroxides: Enhancement of both chemical and stereochemical stabilities of a drug through host-guest interactions, *Chem. Mater.*, 2008, **20**, 5169–5180; (*b*) G.-J. Cui, X.-Y. Xu, Y.-J. Lin, D. G. Evans and D.-Q. Li, Synthesis and UV absorption properties of 5,5′-methylenedisalicylic acid-intercalated Zn−Al layered double hydroxides, *Ind. Eng. Chem. Res.*, 2010, **49**, 448–453.

57 M. K. Ram Reddy, Z. P. Xu and J. C. Diniz da Costa, Influence of water on high-temperature CO_2 capture using layered double hydroxide derivatives, *Ind. Eng. Chem. Res.*, 2008, **47**, 2630–2635.

58 S. Radha and A. Navrotsky, Energetics of CO_2 adsorption on Mg–Al layered double hydroxides and related mixed metal oxides, *J. Phys. Chem. C*, 2014, **118**, 29836–29844.

59 N. D. Hutson, S. A. Speakman and E. A. Payzant, Structural effects on the high temperature adsorption of CO_2 on a synthetic hydrotalcite, *Chem. Mater.*, 2004, **16**, 4135–4143.

60 (*a*) H. Ding, K. Huang, S. Li, L. Xu, J. Xia and M. Li, Flame retardancy and thermal degradation of halogen-free flame-retardant biobased polyurethane materials based on ammonium polyphosphate and aluminium hypophosphite, *Polym. Test.*, 2017, **62**, 325–334; (*b*) M.-J. Xu, G.-R. Xu, Y. Leng and B. Li, Synthesis of a novel flame retardant based on cyclotriphosphazene and DOPO

groups and its application in epoxy resins, *Polym. Degrad. Stab.*, 2016, **123**, 105–114.

61 P. Wen, Q. Tai, Y. Hu and R. K. K. Yuen, Cyclotriphosphazene-based intumescent flame retardant against the combustible polypropylene, *Ind. Eng. Chem. Res.*, 2016, **55**, 8018–8024.

62 V. Rives, Comment on "Direct observation of a metastable solid phase of Mg/Al/CO_3-layered double hydroxide by means of high-temperature *in situ* powder XRD and DTA/TG"[1], *Inorg. Chem.*, 1999, **38**, 406–407.

63 J. Pérez-Ramírez, S. Abelló and N. M. van der Pers, Memory effect of activated Mg–Al hydrotalcite: *In situ* XRD studies during decomposition and gas-phase reconstruction, *Chem.–Eur. J.*, 2007, **13**, 870–878.

64 V. Chandrasekhar and R. Suriya Narayanan, Metalation studies of 3- and 4-pyridyloxycyclophosphazenes: metallamacrocycles to coordination polymers, *Dalton Trans.*, 2013, **42**, 6619–6632.

65 (*a*) L. Zhu, X. Huang and X. Tang, One-pot synthesis of novel poly(cyclotriphosphazene-co-sulfonyldiphenol) microtubes without external templates, *Macromol. Mater. Eng.*, 2006, **291**, 714–719; (*b*) Z. Lu, Y. Weizhong, P. Yang, T. Xiaozhen and H. Xiaobin, Preparation and characterization of novel poly[cyclotriphosphazene-co-(4,4′-sulfonyldiphenol)] nanofiber matrices, *Polym. Int.*, 2006, **55**, 1357–1360.

66 S. Das, S. K. Dash and K. M. Parida, Kinetics, isotherm, and thermodynamic study for ultrafast adsorption of azo dye by an efficient sorbent: Ternary Mg/(Al + Fe) layered double hydroxides, *ACS Omega*, 2018, **3**, 2532–2545.

67 N. T. Whilton, P. J. Vickers and S. Mann, Bioinorganic clays: synthesis and characterization of amino- and polyamino acid intercalated layered double hydroxides, *J. Mater. Chem.*, 1997, **7**, 1623–1629.

68 M. Basharat, M. S. Khan, Y. Abbas, S. Zhang, H. Ma, Z. Wu and W. Liu, Cyclotriphosphazene (P_3N_3) hybrid framework for aggregation induced photocatalytic hydrogen evolution and degradation of rhodamine B, *Mater. Chem. Front.*, 2020, **4**, 3216–3225.

69 A. B. Boscoletto, M. Gleria, R. Milani, L. Meda and R. Bertani, Surface functionalization with phosphazene substrates-part VII. Silicon-based materials functionalized with hexachlorocyclophosphazene, *Surf. Interface Anal.*, 2009, **41**, 27–33.

70 C. Zhu, C. Deng, J.-Y. Cao and Y.-Z. Wang, An efficient flame retardant for silicone rubber: Preparation and application, *Polym. Degrad. Stab.*, 2015, **121**, 42–50.

71 I. Dez and R. De Jaeger, Synthesis and radical polymerization of methacrylate monomers containing cyclotriphosphazene. Thin-layer grafts of their polymers on a poly(vinyl alcohol) surface, *Macromolecules*, 1997, **30**, 8262–8269.

72 L. S. Dake, D. R. Baer, K. F. Ferris and D. M. Friedrich, Ligand and structure effects on the N-P bonds of phosphazenes, *J. Electron Spectrosc. Relat. Phenom.*, 1990, **51**, 439–457.

73 P. Vassileva, V. Krastev, L. Lakov and O. Peshev, XPS determination of the binding energies of phosphorus and nitrogen in phosphazenes, *J. Mater. Sci.*, 2004, **39**, 3201–3202.

74 X. Wang, Y. Hu, L. Song, S. Xuan, W. Xing, Z. Bai and H. Lu, Flame retardancy and thermal degradation of intumescent flame retardant poly(lactic acid)/starch biomaterials, *Ind. Eng. Chem. Res.*, 2011, **50**, 713–720.

75 G. Zhang, L. Wu, A. Tang, B. Weng, A. Atrens, S. Ma, L. Liu and F. Pan, Sealing of anodized magnesium alloy AZ31 with MgAl layered double hydroxides layers, *RSC Adv.*, 2018, **8**, 2248–2259.

76 C. Zhang, J. Yu, L. Xue and Y. Sun, Investigation of γ-(2,3-Epoxypropoxy)propyltrimethoxy silane surface modified layered double hydroxides improving UV ageing resistance of asphalt, *Materials*, 2017, **10**, 78.

77 L. Wu, X. Ding, Z. Zheng, A. Tang, G. Zhang, A. Atrens and F. Pan, Doublely-doped Mg-Al-Ce-$V_2O_7^{4-}$ LDH material film on magnesium alloy AZ31 for anticorrosion, *J. Mater. Sci. Technol.*, 2021, **64**, 66–72.

78 B. Guo, Y. Liu, Q. Zhang, F. Wang, Q. Wang, Y. Liu, J. Li and H. Yu, Efficient flame-retardant and smoke-suppression properties of Mg–Al-layered double hydroxide nanostructures on wood substrate, *ACS Appl. Mater. Interfaces*, 2017, **9**, 23039–23047.

79 K. Wang, D. Meng, S. Wang, J. Sun, H. Li, X. Gu and S. Zhang, Impregnation of phytic acid into the delignified wood to realize excellent flame-retardant, *Ind. Crops Prod.*, 2022, **176**, 114364.

80 K. Zhou, R. Gao and X. Qian, Self-assembly of exfoliated molybdenum disulfide(MoS_2) nanosheets and layered double hydroxide(LDH): Towards reducing fire hazards of epoxy, *J. Hazard. Mater.*, 2017, **338**, 343–355.

81 S. Zhang, Y. Yan, W. Wang, X. Gu, H. Li, J. Li and J. Sun, Intercalation of phosphotungstic acid into layered double hydroxides by reconstruction method and its application in intumescent flame retardant poly(lactic acid) materials, *Polym. Degrad. Stab.*, 2018, **147**, 142–150.